DETECTING DOMINANT PHYTOPLANKTON SIZE CLASSES (MICRO-, NANO- AND PICO-PHYTOPLANKTON) FROM SEAWIFS DATA IN THE MEDITERRANEAN SEA

A. Di Cicco [1,2], M. Sammartino [3], S. Marullo [1], R. Santoleri [3], M. Marcelli [2]

[1]ENEA, Technical Unit Development of Application of Radiation – Frascati, Italy;
[2]Tuscia University - DEB - Laboratory of experimental oceanology and marine ecology - Civitavecchia, Italy;
[3]CNR – Istituto di Scienze dell'Atmosfera e del Clima, Roma, Italy

ABSTRACT

In the recent years several physical, biological and ecological models have been proposed to evaluate the contribution of different Phytoplankton Size Classes (PSCs) or Phytoplankton Functional Types (PFTs) to the total phytoplankton Chlorophyll *a* biomass using satellite data.

In the present work we investigate the potential of such models to describe the spatial distribution and temporal variability of three dominant PSCs in the Mediterranean Sea during the SeaWiFS mission from 1998 to 2010.

Two models due to Brewin et al. (2011) and Hirata et al. (2011) were selected and tested using a Mediterranean subset of the SeaBASS *in-situ* dataset.

The test of the two algorithms indicate that the Brewin models performs better the *in situ* concentration of chlorophyll *a* for all the three size classes (pico-, nano- and micro- phytoplankton) than the Hirata one's.

The subsequent analysis of the SeaWiFS time series suggest that pico-phytoplankton dominates all around the year, with a relative maximum during summer and minima in late autumn – winter in open sea regions not affected by intense spring blooms. Coastal areas instead show the dominance of nano- and micro- phytoplankton, so as in the intense bloom regions in the late winter – spring months.

1. INTRODUCTION

In the last years phytoplankton has represented an important scientific topic owing to its important ecological role in the global Carbon cycle and greenhouse effect.

It plays a key role in the biological carbon pump thanks to its great contribution to the primary production, due to a rapid phytoplankton turnover and to the great extension of the ocean on the earth's surface.

Its bio-geographic distribution, on global and regional scales, is directly influenced by biological, chemical and physical factors, as light, nutrients availability, presence of competitors, predators, pH, all connected to the local dynamic of water masses. These biotic and abiotic factors create a complex system in which the phytoplankton plays a relevant role. Like primary producers, it represents the base of the aquatic system and the first step of the ecological pyramid and the food web.

Phytoplankton community seems to be also an index of environmental anomalies, since it shows new morphological and physiological adjustments whenever the conditions change, like modified size for each specific trophic stadium (Thingstad et al., 1999).

An important descriptor used to understand the community structure is the "cell size", thanks to the relationship between dimensions and pigmentary content, different taxa or stages of growth in the same taxon, photosynthetic efficiency and bio-optical phytoplankton properties (Chisholm, 1992; Organelli et al., 2007; Raven, 1998). The common Phytoplankton Size Classes (PSCs) classification divides phytoplankton community in micro (>20 µm), nano (2-20 µm) and pico (<2 µm) (Sieburth et al., 1978).

In terms of comprehension of biogeochemical function and roles, size structure of phytoplankton communities provides important information such as the knowledge of the community composition itself (Vidussi et al., 2001; Chisholm, 1992; Raven, 1998). It is now known the predominance of the pico-phytoplankton in the oligotrophic water as the larger cells prevail in the rich of nutrients one's, also due to the effect of the molecular diffusion on the feeding of the large cell in very low nutrient condition (Chisholm, 1992). Moreover the pigment "package effect", describing the chlorophyll a efficiency in the light harvesting, is a direct function of the dimension of the cell (Chisholm, 1992; Raven, 1998; Basset et al. 2009).

In some cases several biogeochemical functions correspond to a particular taxon or size class. For example cyanobacteria often represents a large group of pico-planktonic nitrogen-fixers. They are able to fix and use the forms of atmospheric nitrogen, so having a direct impact on the climate change. Again, the principal components of the micro-phytoplankton, diatoms and dinoflagellates, play a dominant role in the Carbon flux into deeper waters (Nair et al. 2008).

Information about the composition of phytoplankton community structure can be obtained from the analysis of *in situ* samples. This approach is based on laboratory techniques like the flow-cytometry (that gives information about the number and the dimensions of the fluorescent cells in a specific water sample volume), HPLC (High Pressure Liquid Chromatography, used to retrieve the composition and concentration of the pigments content of the cells) and the spectrophotometry equipped with the integrative sphere (which provides the pigment light absorption in the visible spectrum). Thanks to these techniques it is possible to collect a considerable dataset of *in situ* dimensional classes measures, which could be used also for other application, like calibration and validation of satellite algorithms.

The composition of the community structure is also reflected in different optical properties of the water column. This allows the use of satellite ocean color data to produce estimate of PSC or PFT using either empirical or semi-analytical models.

Concentration of Total-Chlorophyll a, (TChl a, the sum of Chlorophyll a, divinyl-cholorophyll a, chlorophyllid a, chlorophyll a allomers and epimers), absorption and backscattering are the main variables used by remote sensing data based models to provide synoptic and multi temporal information about phytoplankton distribution.

The combination of *in-situ* and *remote* measures allows us to understand the marine photoautotrophic system in a more complete way.

The paper is organized as follows. In section 2 a brief description of the study area is given. In section 3 we presented the satellite and *in-situ* data and in the 4th one's the algorithms investigated in this work. The determination of the *in-situ* PSCs from the *in-situ* pigments data by a global analytic relation is reported in section 5. After a comparison of the PSCs obtained from the two models versus the *in-situ* data in the section 6, is described the development of new coefficients for the determination of the *in-situ* Mediterranean PSCs (section 7).Results are summarized in section 8, where some directions of future work are also indicated.

2. THE STUDY AREA

The investigation area is the whole Mediterranean Sea (Figure 1). It is a quasi-enclosed sea with dimension, morphology, dynamics and external forcing that make it a "miniature model" for the comprehension of the global ocean complex processes, from the mesoscale to basin-scale (Siokou-Frangou et al.,2010; Lacombe et al., 1981; Robinson and Golnaraghi, 1995).

Respect to the other sea and oceans Mediterranean sea has singular optical properties of the water column, with "oligotrophic waters less blue (30%) and greener (15%) than the global ocean" (Volpe et al., 2007). This peculiarity makes necessary the development of regional bio-optical algorithms, more appropriate for the features of this sea.

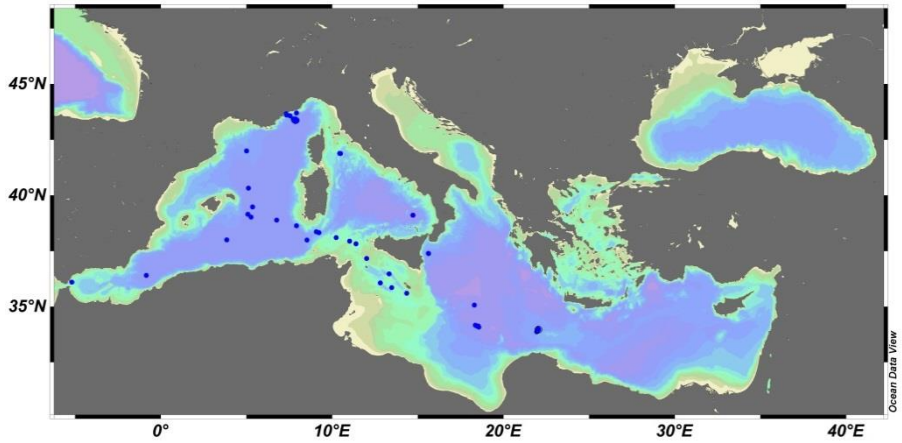

Figure 1 *- Investigation area and location of the SeaBASS in-situ measurements used for this work*

3. THE DATA

3.1 Satellite data

The satellite data used in this work are daily SeaWiFS (Sea-viewing Wide Field-of-view-Sensor) Chlorophyll a estimates, obtained from the MyOcean Ocean Colour Thematic Assembling Centre (MyOcean OC TAC). The specific product we used, case 1 - case 2 merged Chlorophyll (Chl1,2), that takes into account the different optical properties of the offshore and inshore waters. So two different algorithms were applied on the reflectance: the MedOC4 algorithm (Volpe et al., 2007) for the case 1 waters and the Ad4 (Berthon and Zibordi, 2004) for the case 2 one's. For the waters with intermediate features a weighted average of the 2 algorithms were applied, based on the distance between the actual reflectance spectra and the reference reflectance spectra for the case 1 and 2 waters respectively (D'Alimonte et al., 2003).

3.2 *In situ* data

The data used for the determination of the *in-situ* PSCs consist of a Mediterranean subset of the SeaBASS HPLC pigments *in-situ* dataset (Werdell, P.J. and S.W. Bailey, 2005). They are collected in different cruises and in periodical activities of fixed mooring monitoring. In particular this subset consist of data from Propose cruise (1999), Boussole mooring (from 2001 to 2006) and Boum cruise (2008). Figure 1 shows the location of the SeaBASS in situ measurements.

The seven principal diagnostic pigments selected for this work are listed in Table 3.

4. ALGORITHMS DESCRIPTION

4.1 Brewin et al. (2010/2011) algorithm

This is a three component model of PSCs based on an empirical relationship observed between phytoplankton absorption at 443 nm and corresponding pigment, TChl a.

This algorithm is an extension of the Sathyendranath et al. (2001) and Devred et al. (2006).

Sathyendranath et al. (2001) found the equation that better describes phytoplankton absorption as a function of TChl a concentration (Sathyendranath et al., 2001 – Figure 2).

Thanks to the great differences in the optical properties and in the efficiency of harvesting light between the small and large phytoplankton cells (Chisholm, 1992; Raven, 1998; Basset et al., 2009) they obtained an exponential fit function by the assumption that the TChl a concentration is the sum of the concentrations of two distinct in size phytoplankton populations.

Brewin et al. (2010) extended this work to three size classes of phytoplankton populations. The TChl a concentration (C) become the sum of pico- (C_1), nano- (C_2) and micro- phytoplankton (C_3) TChl a concentrations.

$$C = C_1 + C_2 + C_3 \quad (1)$$

As also Devred et al. (2006), they assume that the large cells population is represented by micro-phytoplankton, and the small cells population is the sum of the nano- and pico- phytoplankton. So the Sathyendranath et al. (2001) model becomes, for three components:

$$C_{1,2} = C_{1,2}^{m}\left[1 - exp\left(-S_{1,2}C\right)\right] \quad (2)$$

$$C_1 = C_1^{m}[1 - exp(-S_1 C)] \quad (3)$$

where $C_{1,2}^{m}$ and C_1^{m}, are the asymptotic maximum values for the dependent variables $C_{1,2}$, C_1, and $S_{1,2}$ and S_1 represent their initial slope respectively of the Sathyendranath et al. (2001) finally fit equation.

Known this quantities its simple to derive C_2 and C_3 from:

$$C_2 = C_{1,2} - C_1 \quad (4)$$

$$C_3 = C - C_{1,2} \quad (5)$$

These algorithms and their fixed parameters (Table 1) are derived from a global dataset of TChl a measures.

Population	Maximum C for given population	Initial slope
Nano- + Pico- phytoplankton	*0.775 mgm^{-3}* $(\mathrm{C}_{1,2}^{\mathrm{m}})$	*1.152* $(S_{1,2})$
Pico- phytoplankton	*0.146 mgm^{-3}* $(\mathrm{C}_{1}^{\mathrm{m}})$	*5.118* (S_1)

***Table 1**. Parameters used in eq. (2) and (3) (from Brewin et al., 2011)*

By the equation (3),(4) and (5), dividing for C, we obtained the fractions of each size classes (micro- nano- and pico- phytoplankton) expressed in terms of absolute values respect to the TChl a.

4.2 Hirata et al. (2011) algorithm

Hirata model is based on the synoptic relationship between diagnostic pigments concentration representative of the PSCs and Total Chlorophyll a concentration.

Hirata et al. 2011 applied the Diagnostic Pigment Analysis (DPA), originally proposed by Vidussi et al. (2001) and afterwards modified by Uitz et al. (2006) (Table 2), to a global HPLC pigments dataset, to determine the relative abundance of each size classes respect to the satellite derived TChl a. So these algorithms are obtained:

$$\boldsymbol{Micro} = [0.9117 + \exp(-2.7330 * \mathrm{x} + 0.4003)]^{-1} \quad (6)$$

$$\boldsymbol{Nano} = [1 - \mathrm{Micro} - \mathrm{Pico}] \quad (7)$$

$$\boldsymbol{Pico} = -\left[0.1529 + \exp(1.0306 * \mathrm{x} - 1.5576)\right]^{-1} - 1.8597 * \mathrm{x} + 2.9954 \quad (8)$$

where x is the $log_{10}(Chl\ a)$. Using the technique of DPA, Hirata is able to recognize also a several taxa associated to a specific Phytoplankton Functional Types (PFTs).

***Table 2**. PSCs and PFTs represented by the combination of diagnostic pigments (from Hirata et al. 2011)*

PSCs/PFTs	Diagnostic Pigments	Estimation Formula
Microplankton (>20 µm)*[1]	Fucoxanthin **(Fuco)**, Peridinin **(Peri)**	1.41 (Fuco+Peri)/ TChl *a* *[2]
Diatoms	**Fuco**	1.41 Fuco/ TChl *a* *[2]
Dinoflagellates	**Peri**	1.41 Perid/ TChl *a* *[2]
Nanoplankton (2-20 µm)*[1]	19'Hexanoyloxy-fucoxanthin **(19'Hex)** Total Chlorophyll-*b* **(TChl-*b*)** 19'Butanoyloxy-fucoxanthin **(19'But)** Alloxanthin **(Allo)**	(X_n*1.27 19'Hex + 1.01 TChl *b* + 0.35 19'But + 0.60 Allo)/ TChl *a* *[3]
Green algae	**TChl *b***	1.01 TChl-*b*/ TChl *a* *[2]
Prymnesiophytes*[4] (Haptophytes)	**19'Hex, 19'But**	Nano – Green algae ***[4]**
Picoplankton (0.2-2 µm)*[1]	Zeaxanthin **(Zea)**, **19'He**x, **TChl *b***	(0.86 Zea + Y_p 1.27 Hex)/ TChl *a* *[3]
Prokaryotes	**Zea**	0.86 Zea/ TChl *a* *[2]
Pico-eukaryotes	**19'Hex**, **TChl *b***	Pico – Prokaryotes
Prochlorococcus sp.	Divinyl Chlorophyll a **(DVChl *a*)**	0.74 DVChl- a /TChl a

*[1] Sieburth et al. (1978)
*[2] TChl a = 1.41 Fuco + 1.41 Perid + 1.27 Hex + 0.6 Allo + 0.35 But + 1.01 Chl-*b* + 0.86 Zea = Chl-a (Uitz et al., 2006)
*[3] X_n= proportion of nanoplankton contribution in 19'Hex; Y_p = proportion of picoplankton in 19'Hex, (Brewin et al., 2010).
*[4] The contributions of Allo to nanoplankton were only a few percent in Hirata et al. (2011) data set, so Haptophytes were approximated to Nano minus Green Algae.

5. PSCs DETERMINATION FROM "*IN-SITU*" DATA

In order to test the performances of the two global models mentioned above on the Mediterranean Sea characteristics, it's necessary the determination of PSCs from *in-situ* data.

For this purpose we have referred to Vidussi et al. (2001) for the definition of size structure indices, based on the taxonomic meaning of several accessory pigments that can be determined, together with Total Chlorophyll a, by HPLC technique. This study identifies from previous works (Gieskes et al., 1988; Goericke and Repeta, 1993; Claustre and Marty, 1995), seven principal Diagnostic Pigments ($\boldsymbol{DP}$), able to outline the size structure of the whole community (Table 3). "$\sum \boldsymbol{DP}$" is the sum of all seven $\boldsymbol{DP}$ concentrations (mg m^{-3}):

$$\sum DP = [Zea] + [TChlb] + [Allo] + [19'\,Hex\text{-}fuco] + [19'\,But\text{-}fuco] + [Fuco] + [Peri] \quad (9)$$

Diagnostic Pigments	Abbreviations	Taxonomy	PSCs
Fucoxanthin	Fuco	Diatoms	Micro (> 20 µm)
Peridinin	Peri	Dinoflagellates	Micro (> 20 µm)
19'-hexanoyloxyfucozanthin	19' Hex-fuco	Chromophytes and nanoflagellates	Nano (2-20 µm)
19'-butanoyloxyfucoxanthin	19' But-fuco	Chromophytes and nanoflagellates	Nano (2-20 µm)
Alloxanthin	Allo	Cryptophytes	Nano (2-20 µm)
Chlorophyll *b* + divinyl-chlorophyll *b*	TChl*b*	Green flagellates and prochlorophytes	Pico (<2 µm)
Zeaxanthin	Zea	Cyanobacteria and prochlorophytes	Pico (< 2 µm)

Table 3 *- Diagnostic Pigments used in this work and their reference taxonomic and size classes (*Vidussi et al., 2001; Uitz et al., 2006).

The biomass fraction (f) associated with each size class is defined as:

$$\boldsymbol{f_{pico}} = ([Zea] + [TChlb])/\sum DP \quad (10)$$

$$\boldsymbol{f_{nano}} = ([Allo] + [19'\,Hex\text{-}fuco] + [19'\,But\text{-}fuco])/\sum DP \quad (11)$$

$$\boldsymbol{f_{micro}} = ([Fuco] + [Peri]/\sum DP \quad (12)$$

In Vidussi et al. (2001) $\sum DP$ is considered a valid estimator of TChl a, thanks to a significant linear regression found between the two parameters, but they assume an equal weight of each diagnostic pigment to TChl a, not taking into account the variation in the $\sum DP/TChla$ ratio due to different species and physiological state (as already point out by Vidussi et al, 2001).

In order to obtain a more accurate quantification of each size class in terms of TChl a, Uitz et al. (2006) following the previous work of Gieskes et al. (2008), carried out a multiple regression analysis of [TChl a] and the concentration of the most important accessory pigments. This study provides the best estimates of the seven Total Chlorophyll a - diagnostic pigments ratio $(TChla/DP)$ for a global data set:

$$TChla = 0.86[Zea] + 1.01[TChlb] + 0.60[Allo] + 1.27[19'\,Hex\text{-}fuco] + 0.35\left[19'\,But\text{-}Fuco\right] + 1.41[Fuco] + 1.41[Peri] \quad (13)$$

According to Uitz et al. (2006) the fractions of the Chlorophyll a concentration associated with each of the three phytoplanktonic classes are:

$$\boldsymbol{f_{pico}} = (0.86[Zea] + 1.01[TChlb])/TChla \quad (14)$$

$$\boldsymbol{f_{nano}} = (0.60[Allo] + 1.27[19'\,Hex\text{-}fuco] + 0.35[19'\,But\text{-}fuco])/TChla \quad (15)$$

$$\boldsymbol{f_{micro}} = (1.41[Fuco] + 1.41[Peri]/TChla \quad (16)$$

These relationships have been applied to a Mediterranean subset of the SeaBASS HPLC pigment dataset (Werdell, P.J. and S.W. Bailey, 2005) (Figure 1) to obtain *in-situ* concentrations of TChl a

of each PSCs for the calibration and/or validation of an algorithm that performs better the optical properties of the Mediterranean Sea.

For this work we take into account the whole complete *in-situ* data for the first 40 m of the water column.

It should be noted, as reported previously by Vidussi et al. (2001), that the phytoplankton grouping based on the auxiliary pigments concentration not strictly reflects the true phytoplankton size. This is because in the same taxonomic class there are species of different dimensions that may be enclosed in more than one size classes. The same may occur in a single species at different stages of growth. Moreover some taxonomic pigment may be in small concentrations in other minor groups. Nevertheless this classification it's a good conventional approximation, taking into account several investigations about the typical off shore composition of phytoplankton Mediterranean community (Siokou-Frangou et al., 2009; Vidussi et al.,2001). Using the HPLC determination of the PSCs is important to fix that when we speak of micro- we referred to Diatoms and Dinoflagellates in general, nano- includes all the Cryptophytes, nanoflagellates and Chromophytes and pico- phytoplankton is referred to Cyanobacteria, green tiny flagellates and Prochlorophytes (Table 3).

6. PHYTOPLANKTON SIZE CLASSES: MODELS versus *IN-SITU* DATA

In the matching of the size-specific fractional contributions to the Total Chlorophyll a concentration derived from *in-situ* diagnostic pigments versus the PSCs obtained by the Brewin and Hirata models (Figure 2 and 3 respectively), both algorithms show a general good qualitative performances when applied to the Mediterranean SeaBASS subset (fig. 2 and 3 on the right, respectively) compared with the original global case study (Figure 2 and 3 on the left, respectively).

In particular, for the Mediterranean data, the plots indicate that Hirata underestimate the micro-phytoplankton (Figure 3, a) and slightly overestimate the pico- phytoplankton (Figure 3, c). Instead a good agreement is pointed out between the Hirata model and the nano size class (Figure 3, b). Brewin, on the other hand, performs better the micro-component (Figure 2, a) but underestimate, slightly, the pico-phytoplankton (Figure 2, d) at lower TChl a value than Hirata and strongly the whole nano component (Figure 2, c): both models show both strengths that weaknesses for the Mediterranean

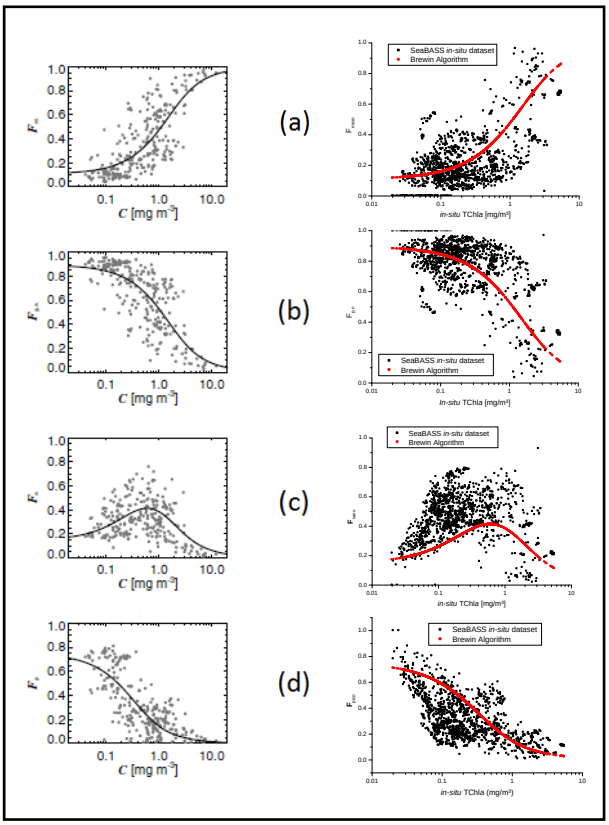

Figure 2 *- Brewin model versus PSCs from in-situ measures (global dataset on the left, from Brewin et al, 2011, Mediterranean SeaBASS dataset on the right) for micro (a), nano&pico (b), nano (c) and pico (d) phytoplankton.*

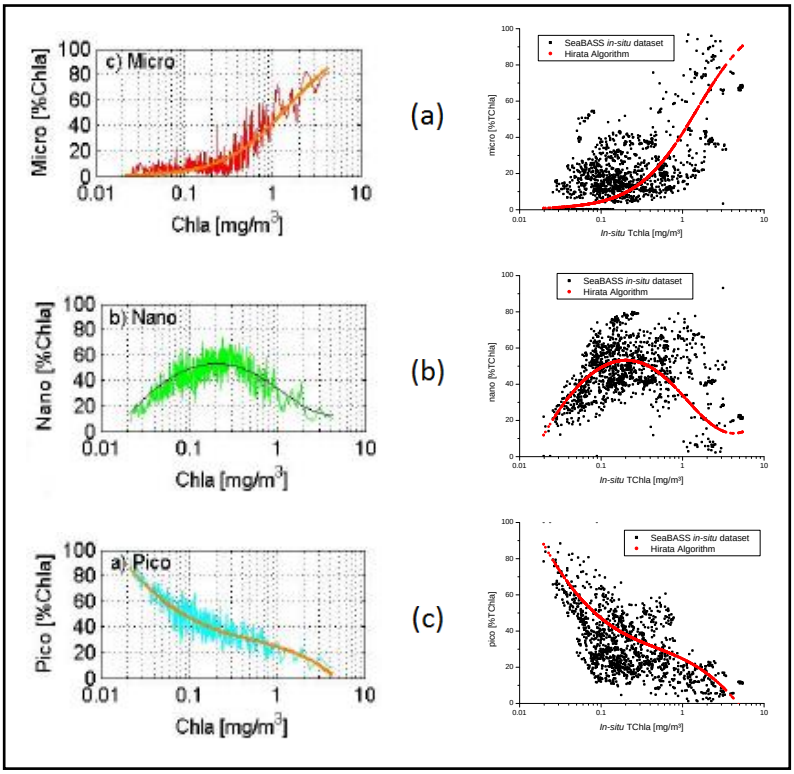

Figure 3 *- Hirata model versus PSCs from in-situ measures (global dataset on the left, from Hirata et al, 2011, Mediterranean SeaBASS dataset on the right) for micro (a), nano (b) and pico (c) phytoplankton.*

7. MEDITERRANEAN DETERMINATION OF PIGMENT COEFFICIENTS

The Uitz et al. (2006) algorithms used in this first step to determine the TChl a fraction of each PSCs are based on a multiple regression analysis applied on a global dataset. To better test the performances of the Brewin and Hirata models, a new multiple regression analysis on the SeaBASS pigment dataset was performed in this work in order to recalculate new coefficients (Table 4) that best reflect the pigment composition of the Mediterranean phytoplankton community.

Pigments Biomarker	Uitz coefficients	Recalculate coefficients
Fuco	1.41	1.740
Peri	1.41	1.172
19' Hex-fuco	1.27	0.861
19' But-fuco	0.35	0.405
Allo	0.60	2.088
TChl *b* *	1.01	1.624
Zea	0.86	1.999

Table 4 *- Comparison between Uitz et al. 2006 global coefficient and Mediterranean coefficient from this work for the in-situ determination of PSCs.*

On the basis of this analysis the best estimate of Total Chlorophyll a - diagnostic pigments ratio ($\sum DP/TChla$) for a Mediterranean data set is:

$$TChla = 1.999[Zea] + 1.624[TChlb] + 2.088[Allo] + 0.861[19'\,Hex\text{-}fuco]$$
$$+0.405\left[19'\,But\text{-}Fuco\right] + 1.74[Fuco] + 1.172[Peri] \quad (17)$$

and the new algorithms for the determination of the contribution of each PSCs to the TChl a are:

$$\boldsymbol{f_{pico}} = (1.999[Zea] + 1.624[TChlb])/TChla \quad (18)$$

$$\boldsymbol{f_{nano}} = (2.088[Allo] + 0.861[19'\,Hex\text{-}fuco] + 0.405[19'\,But\text{-}fuco])/TChla \quad (19)$$

$$\boldsymbol{f_{micro}} = (1.74[Fuco] + 1.172[Peri]/TChla \quad (20)$$

Applying these new algorithms to the Mediterranean SeaBASS *in-situ* subset the matching between the two models and the in-situ PSCs change, pointing out an unequivocal better performance of Brewin algorithm than Hirata one's for all Phytoplankton dimensional classes (Figure 4).

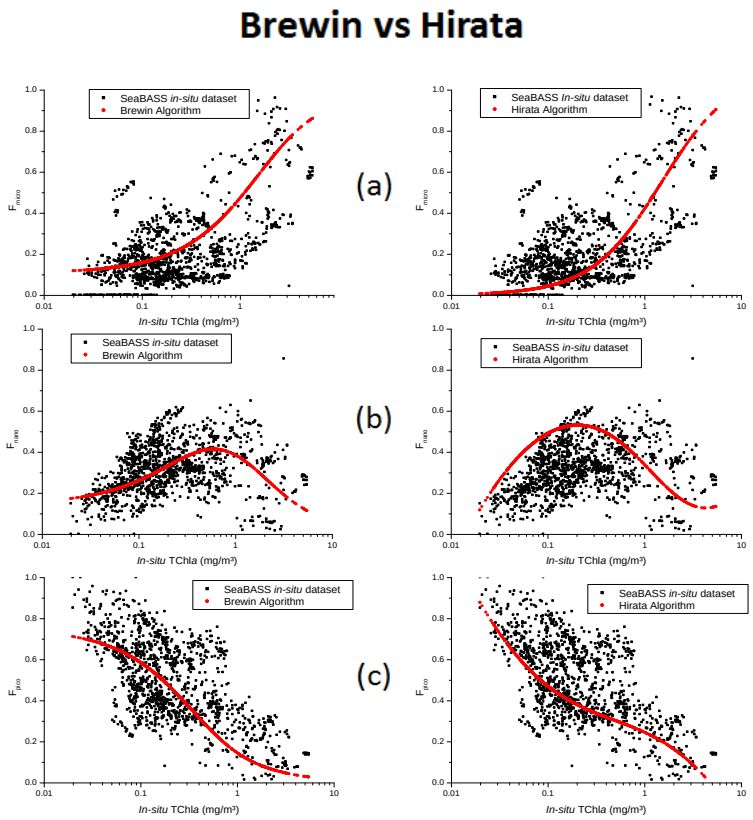

Figure 4 *– Brewin (on the left) and Hirata (on the right) models versus PSCs obtained applying recalculated coefficients on the Mediterranean SeaBASS in-situ measures for micro (a), nano (b) and pico (c) phytoplankton.*

These consideration are supported by basic statistical analysis parameters: Mean Bias Error (MBE), Root Mean Square Error (RMSE) and Pearson correlation coefficient (R),

$$MBE = \frac{\sum_{i=1}^{N}(x_i - y_i)}{N}$$

$$RMSE = \sqrt{\frac{\sum_{i=1}^{N}(x_i - y_i)^2}{N}}$$

$$R = \frac{\sum_{i=1}^{N}(x_i - \bar{x})(y_i - \bar{y})}{\sqrt{\sum_{i=1}^{N}(x_i - \bar{x})^2}\sqrt{\sum_{i=1}^{N}(y_i - \bar{y})^2}}$$

where x_i represent the PSCs estimated by the model, y_i the PSCs estimated by Diagnostic Pigments, N is the total number of the matchup data and the bar indicate the arithmetic average (R is dimensionless, MBE and RMSE have the same dimension of *x* and *y*). These parameters was calculated for Brewin and Hirata models both with old (Uitz et al., 2006) that new coefficients (Table 5).

	Mean Bias Error				Root Mean Square Error			
	Brewin (Uitz)	Brewin (Us)	Hirata (Uitz)	Hirata (Us)	Brewin (Uitz)	Brewin (Us)	Hirata (Uitz)	Hirata (Us)
F_{micro}	0.0411	**0.0525**	-0.0549	-0.0435	0.1517	**0.1523**	0.1697	0.1634
F_{nano}	-0.1602	**-0.0088**	-0.0221	0.1293	0.2118	**0.1128**	0.1384	0.1902
F_{pico}	0.1191	**-0.0437**	0.0770	-0.0858	0.2065	**0.1727**	0.1526	0.1728

Table 5 *– Mean bias Error and Root Mean Square Error between PSCs obtained by the models and PSCs from Diagnostic Pigments calculated for Brewin and Hirata models with old (Uitz et al., 2006) and new coefficients ("+" represents overestimation, "-" underestimation).*

In particular, MBE and RMSE show that the in situ PSCs obtained with the new Mediterranean coefficients performs better with the Brewin model than the Hirata one's. Furthermore, the error for the Brewin model versus the PSCs with new coefficients is more uniform and reasonable for the whole dimensional classes than the error obtained from Brewin and Hirata models with the old coefficients (Table 5).

Pearson Correlation Coefficient (R)				
	Brewin (Uitz)	Brewin (Us)	Hirata (Uitz)	Hirata (Us)
F_{micro}	0.6185	**0.6329**	0.6207	0.6344
F_{nano}	0.3722	**0.3912**	0.4632	0.2387
F_{pico}	0.5469	**0.6195**	0.6412	0.6483

Table 6 *– Pearson Correlation Coefficient between PSCs obtained by the models and PSCs from Diagnostic Pigments calculated for Brewin and Hirata models with old (Uitz et al., 2006) and new coefficients.*

So the Brewin algorithm was selected for this work and climatological maps (Figures 5 and 6) and histograms (Figure 7) of Total Chlorophyll a concentration and biomass associated with each size class have been produced for the whole SeaWIFS era (1998-2010), giving as input to the model the case 1-case2 merged chlorophyll maps produced by CNR in the MyOcean OC TAC.

8. RESULTS AND PERSPECTIVES

8.1 Mediterranean PSCs distribution

Climatological maps (Figure 5 and 6) and histograms (Figure 7) are developed in order to study the spatial and temporal distribution of the three size classes micro-, nano- and pico-phytoplankton.

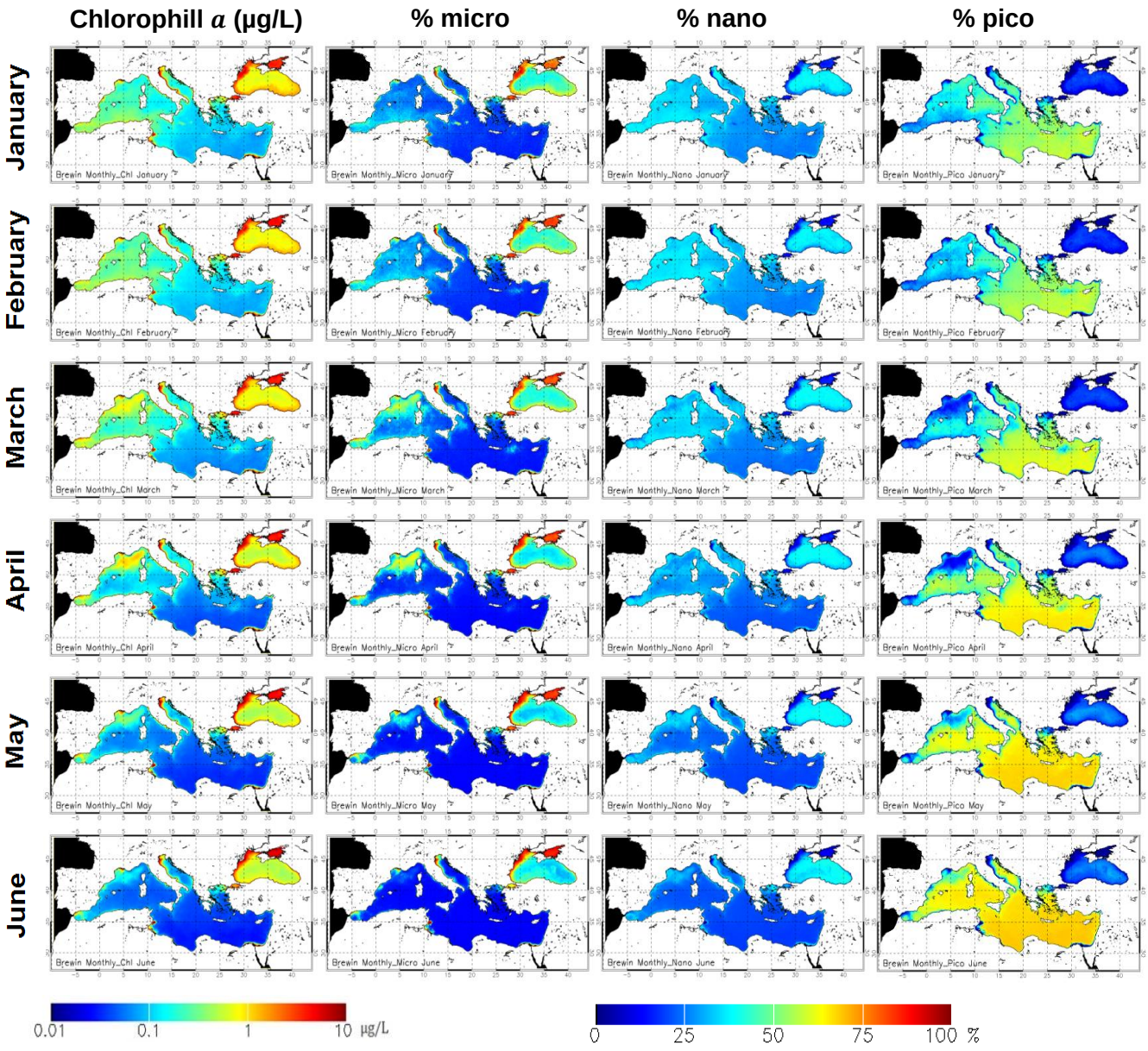

Figure 5 *- Climatological maps, from January to June, for the SeaWIFS era (1998-2010)*

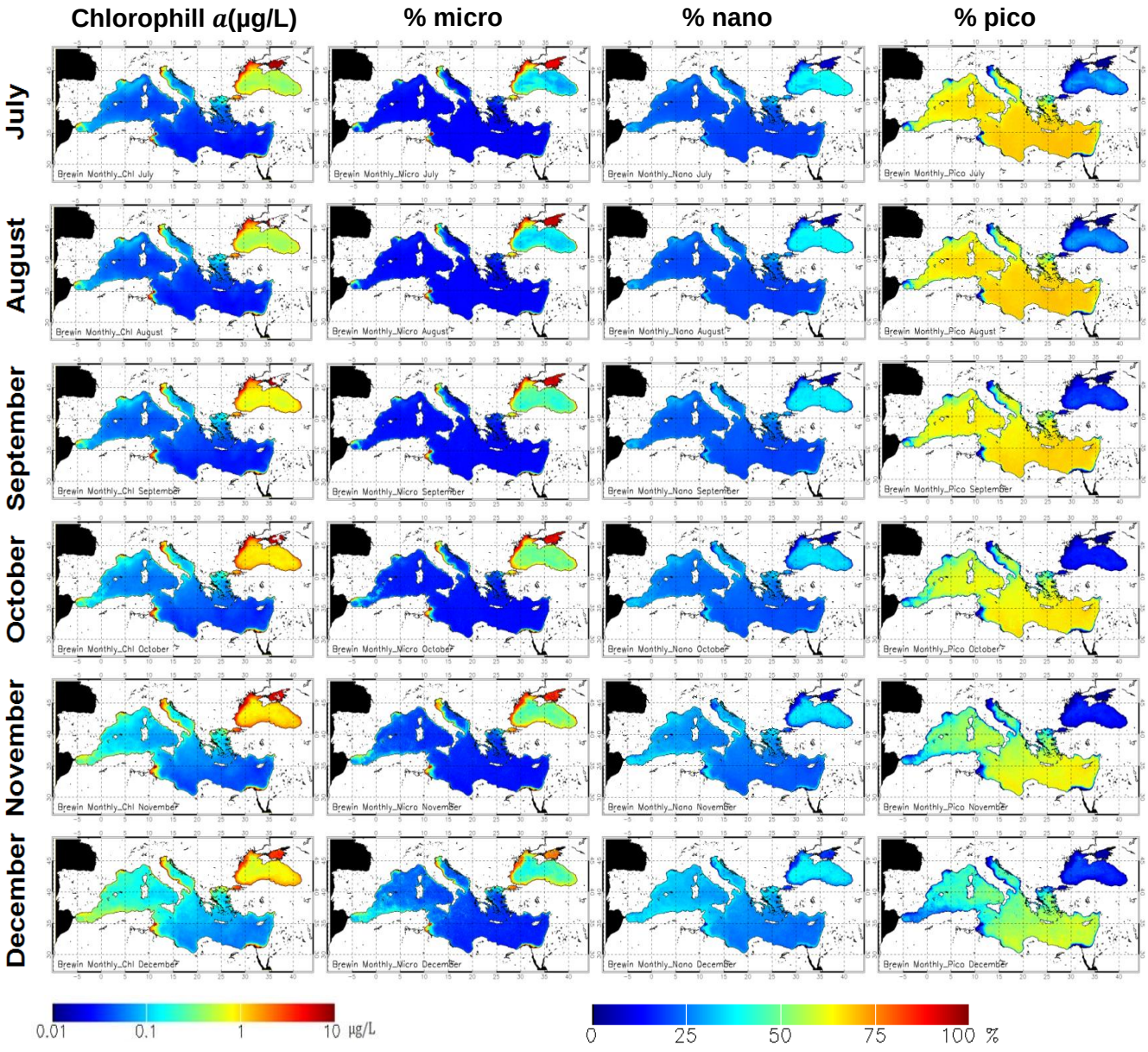

Figure 6 *- Climatological maps, from July to December, for the SeaWIFS era (1998-2010)*

The maps give information about the “relative proportion” of micro-, nano- and pico- phytoplankton for each Total Chlorophyll a concentration in the first optical depth. Showing percentages, in their evaluation we have to take into account that they are mutually compensatory.

The analysis of the SeaWiFS time series suggest that pico-phytoplankton dominates the open sea regions not affected by intense spring blooms all around the year, with maxima relative values during summer and minima in late autumn and winter. This agrees with the work of Siokou-Frangou et al. (2010), whereby low biomass value regions, in the Mediterranean Sea as in the most oligotrophic areas in general, are characterized by the dominance of cyanobacteria, prochlorophytes and tiny flagellates, typical pico-phytoplankton components. In these areas micro- (Diatoms and Dinoflagellates) and nano- (Cryptophytes, nanoflagellates and Chromophytes) phytoplankton show an increasing in the late winter - spring, typical bloom period for the Mediterranean latitudes, but the smallest fraction of the phytoplankton represents however the principal component of the Total Chlorophylla a (Figure 7, b,c,h,i). Pico is very abundant all the year especially in Levantine basin, but in summer it reaches higher relative values, as 65-70% of the total biomass, in the whole Mediterranean basin.

Different is the case of the coastal and intense bloom regions that show a more complex situation.

In the coastal areas the dominance in the Total Chlorophyll a of nano- and micro- phytoplankton features all the year, with micro representing the principal component and nano follows the same trend (Figure 7, d). This is, often, due to the presence of nutrients rich waters influenced by the discharge of big rivers, heavy precipitation’s events and snowmelt (Struglia et al., 2004).

In the intense spring bloom regions, pico- nano- and micro- components of the Total Chlorophyll a concentration show similar values almost all the year (generally with a pico- predominance), except in the late winter - spring months, in which micro- and nano- TChl a reach higher concentrations, above all in the western basin (Figure 7, g) but especially in the Alboràn Sea and Liguro-Provençal basin (Figure 7, f). Here, together with the Rodhes’s gyre for the eastern MS (Figure 5, March), microphytoplankton contribution to the chlorophyll a becomes strongly dominant, also on the nanoplankton, that anyway shows the same trend of micro, showing high values. It’s important underlines the confirmed relation between higher values of Total Chlorophyll a and the predominance of the larger phytoplankonic components (Figure 5, March or April; Figure 7, f) and more oligotrophic waters and pico-phytoplankton relative dominance (Figure 6, July or August; Figure 7 c, h, i), in agreement with Malone (1980) and Chisholm (1992).

In general nano distribution seems to be constant/consistent during the whole year, with high values in spring and late autumn/winter months, and lower in summer, as nearly to micro.

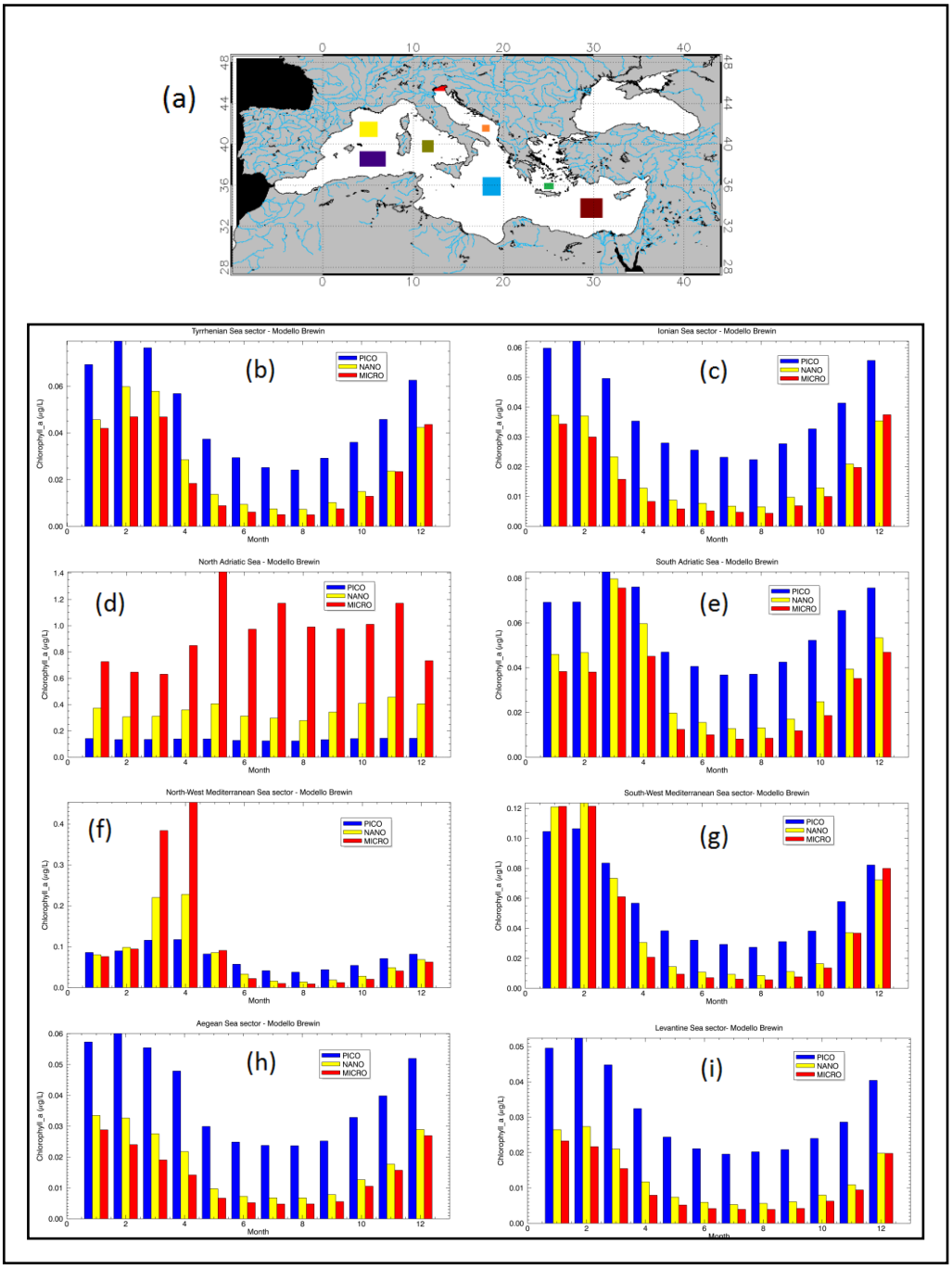

Figure 7 *- Seasonal variation of Phytoplankton Size Classes in specific sectors (a) of the Mediterranean Sea: Tyrrhenian Sea (b), Ionian Sea (c), North Adriatic Sea (d), South Adriatic Sea (e), North-western Mediterranean Sea (f),South-western Mediterranean Sea (g), Aegean Sea (h) and Levantine Sea (i) sectors.*

8.2 . Conclusions and perspectives

In the present work we have analyzed two of the principal global algorithms for the determination of the PSCs by satellite techniques, with the aim to investigate the Phytoplankton Size Classes distribution in the Mediterranean Sea. Brewin model and Hirata one's were tested by a consistent Mediterranean *in-situ* pigment subset (from SeaBASS dataset). On the basis of previous works (Gieskes et al., 2008; Vidussi et al. 2001; Uitz et al., 2006) new cofficients for the determination of the *in-situ* Mediterranean PSCs were developed by a multiple regression analysis. Comparing the two models with the *in-situ* data, statistical analysis shows that Brewin algorithm perform better than the Hirata one's. So we applied the Brewin model to a reanalysis of daily Chlorophyll a estimates, carried out by the MyOcean OC TAC, for the entire SeaWiFS mission (1998 - 2010).

The products obtained, displayed by climatological maps and histograms, show the predominance, in the first optical depth, of picophytoplankton on micro and nano components of the TChl a all around the year in the most oligotrophic areas or periods. The TChl a in coastal regions is always dominated by microphytoplankton. Intense bloom spring areas show an alternation. The pico is the principal component almost all year, except in the late winter – spring period in which micro and nano contribution to the TChl a reach higher concentration. These considerations are in agreement with the main works on the Mediterranean phytoplankton distribution (Siokou-Frangou et al., 2010; Uitz et al., 2012).

These results validate and support the importance of the satellite techniques also in the synoptic identification of the phytoplankton dimensional groups. Although a more accurate understanding of the phytoplankton community requires a discrimination at "taxonomic classes" level, (direction in which it's progressing, as already Alvain et al., 2005; Sathyendranath et al., 2004), is well scientifically recognized the strong influence of the factor "size" on the entire physiology of phytoplankton, weighed also from a biogeochemical point of view (Nair et al., 2008).

Future developments of this work want to take into account other theoretical algorithms (Alvain et al., 2005; Kostadinov et al., 2009; Sathyendranath et al., 2004) and a more ecological approach (Raitsos et al., 2008). The goal is to identify the more robust algorithm, able to outline the Mediterranean phytoplankton community in a more detailed way, with the aim to contribute at the understanding of its dynamics.

With the same objective, through the organization of several oceanographic cruises, we are collecting an *in-situ* independent dataset required to validate the final algorithm.

Our intent is to extend this investigation also to MODIS and MERIS data, in view of the ESA – Ocean Colour Climate Change, initiative that will realize an unique and consistent Ocean Colour time series.

9. REFERENCES

Alvain S., Moulin C., Dandonneau Y., Bréon FM. (2005) Remote sensing of phytoplankton groups in case 1 waters from global SeaWiFS imagery. Deep-Sea Res I 52: 1989-2004.

Basset, A., Sangiorgio, F. and Sabetta, L. (2009).. Nuovi approcci metodologici per la classificazione dello stato di qualità degli ecosistemi acquatici di transizione. Metodologie ISPRA

Berthon, J.-F., Zibordi, G., 2004. Bio-optical relationships for the northern Adriatic Sea. Int. J. Remote Sens., 25, 1527-1532

Brewin, R.J.W., Sathyendranath, S., Hirata, T., Lavender, S.J., Barciela, R. and Hardman-Mountford, N.J. (2010). A three-component model of phytoplankton size class from satellite remote sensing. Ecological Modelling, 221(11): 1472-1483. doi: 10.1016/j.ecolmodel.2010.02.014.

Brewin, R. J. W., Devred, E., Sathyendranath, S., Lavender, S. J. and Hardman-Mountford, N. J. (2011). Model of phytoplankton absorption based on three size classes. Applied Optics, 50(22): 4353-4364. doi: 10.1364/AO.50.004535.

Chisholm, S. W. (1992). Phytoplankton size. In: Primary Productivity and Biogeochemical Cycles in the Sea. Edited by P.G. Falkowski and A.D. Woodhead, Plenum Press, New York.

Claustre, H. and Marty, J. C. (1995). Specific phytoplankton biomasses and their relation to primary production in the Tropical North Atlantic. Deep Sea Research Part I: Oceanographic Research Papers, 42: 1475-1493.

D'Alimonte, D., Mélin, F., Zibordi, G., Berthon, J.-F. (2003). Use of the novelty detection technique to identify the range of applicability of the empirical ocean color algorithms. IEEE Trans. Geosci. Remote Sens., 41: 2833-2843.

Devred, E., Sathyendranath, S., Stuart, V., Maass, H., Ulloa, O., and Platt, T. (2006). A two-component model of phytoplankton absorption in the open ocean: Theory and applications, J. Geophys. Res., 111, C03011, doi:10.1029/2005JC002880.

Gieskes, W. W. C., Kraay, G. W., Nontji, A, Setiapermana, D. and Sutomo (1988). Monsoonal alternation of a mixed and a layered structure in the phytoplankton of the euphotic zone of the Banda Sea (Indonesia): A mathematical analysis of algal pigment fingerprints, Neth. J. Sea Res., 22(2): 123–137

Goericke, R. and Repeta, D.J. (1993). Chlorophylls a and b and divlnyl chlorophylls a and b in the open subtropical North Atlantic Ocean. Mar. Ecol. Prog. Ser. 101: 307-313

Hirata, T., Hardman-Mountford, N.J., Brewin, R.J.W., Aiken, J., Barlow, R., Suzuki, K., Isada, T., Howell, E., Hashioka, T., Noguchi-Aita, M. and Yamanaka, Y. (2011). Synoptic relationships between surface Chlorophyll-a and diagnostic pigments specific to phytoplankton functional types, Biogeosciences, 8: 311-327, doi: 10.5194/bg-8-311-2011.

Kostadinov, T.S., Siegel, D.A., Maritorena, S. (2009). Retrieval of the particle size distribution from satellite ocean color observations. Journal of Geophysical Research 114, C09015.

Lacombe, H., Gascard, J. C., Gonella J. and Bethoux, J. P. (1981). Response of the Mediterranean to the water and energy fluxes across its surface, on seasonal and interannual scales. Oceanologica Acta, 4: 247–255.

Malone, T. C. (1980). Algal size, p. 433-463. *In* I. Morris [ed], The physiological ecology of phytoplankton. Univ. California.

Nair, A., Sathyendranath, S., Platt, T., Morales, J., Stuart, V., Forget, M.H., Devred, E. and Bouman, H. (2008). Remote sensing of phytoplankton functional types. Remote Sensing of Environment 112: 3366-3375.

Organelli, E., Nuccio, N., Massi, L., 2007. Individuazione dei principali gruppi fitoplanctonici in base al loro contributo di assorbimento e retrodiffusione nella riflettanza. Ecologia Limnologia e Oceanografia: quale futuro per l'ambiente: 181-187. Ancona, 17 - 20 settembre 2007.

Raitsos, D. E., Lavender, S. J., Maravelias, C. D., Haralabous, J., Richardson, A. J. and Reid, P. C. (2008). Identifying four phytoplankton functional types from space: An ecological approach. Limnol. Oceanogr., 53(2): 2008, 605–613

Raven, J. A. (1998). Small is beautiful. Functionnal Ecology, 12: 503-513.

Robinson, A. R. and Golnaraghi, M. (1995). The Physical and dynamical oceanography of the Mediterranean sea. In Malanotte-Rizzoli, P. and Robinson, A. R. editors, Ocean Processes in Climate Dynamics: Global and Mediterranean Examples: 255–306. NATO-ASI, Kluwer Academic Publishers, Dordrecht, The Netherlands.

Sathyendranath, S., Stuart, V., Cota, G., Maas, H. and Platt, T. (2001). Remote sensing of phytoplankton pigments: a comparison of empirical and theoretical approaches. International Journal of Remote Sensing 22: 249–273.

Sathyendranath, S., Watts, L., Devred, E., Platt, T., Caverhill, C., Maass, H. (2004). Discrimination of diatoms from other phytoplankton using ocean-colour data. Marine Ecological Progress Series 272: 59–68.

Schlitzer, R., Ocean Data View, http://odv.awi.de, 2013.

Siokou-Frangou, I., U. Christaki, M. G. Mazzocchi, M. Montresor, M. Ribera d'Alcalá, D. Vaqué, and A. Zingone (2010), Plankton in the open Mediterranean Sea: A review, Biogeosciences, 7: 1543–1586, doi:10.5194/bg-7-1543.

Struglia, M., V., Mariotti, A. and Filograsso, A., (2004). River Discharge into the Medtierranean Sea: Climatology and aspects of the Observed variability, Journal of climate, 17: 4740-4751.

Thingstad F.T. and Rassoulzadegan F. (1999). Conceptual models for the biogeochemical role of the photic zone microbial food web, with particular reference to the Mediterranean Sea. Prog. Oceanogr. 44: 271- 286.

Uitz, J., Claustre, H., Morel, A., and Hooker, S. B. (2006). Vertical distribution of phytoplankton communities in open ocean, An assessment based on surface chlorophyll, J. Geophys. Res., 111, C08005, doi:10:1029/2005JC003207.

Uitz, J., Stramski D., Gentili B., F. D'Ortenzio F., and Claustre H. (2012), Estimates of phytoplankton class-specific and total primary production in the Mediterranean Sea from satellite ocean color observations, Global Biogeochemical Cycles, 26, GB2024, doi:10.1029/2011GB004055.

Vellucci, V. (2007). Optical properties in the Mediterranean open waters, (Universita degli studi di Napoli “Federico II). PhD Thesis, pp.156.

Vidussi, F., Claustre, H., Manca, B. B., Luchetta, A., and Marty, J. (2001). Phytoplankton pigment distribution in relation to upper thermocline circulation in the eastern Mediterranean Sea during winter, J. Geophys. Res., 106 (C9): 19939–19956.

Volpe, G., Santoleri, R., Vellucci, V., Ribera d'Alcalà, M., Marullo, S. and D'Ortenzio, F. (2007). The colour of the Mediterranean Sea: Global versus regional biooptical algorithms evaluation and implication for satellite chlorophyll estimates. Remote Sensing of Environment 107: 625-638.

Werdell, P.J. and S.W. Bailey , 2005: An improved bio-optical data set for ocean color algorithm development and satellite data product validation. Remote Sensing of Environment , 98(1): 122 140.